View metadata, citation and similar papers at core.ac.uk

brought to you by CORE

provided by NASA Technical Reports Server

3 1176 00071 4973

NATIONAL ADVISORY COMMITTEE FOR AERONAUTICS

TECHNICAL NOTE

No. 1193

EFFECT OF PRODUCT OF INERTIA ON LATERAL STABILITY

By Leonard Sternfield

Langley Memorial Aeronautical Laboratory
Langley Field, Va.

LIBRARY COPY
2 1993
LANGLEY RESEARCH CENTER
LIBRARY NASA
HAMPTON, VIRGINIA

Washington
March 1947

NATIONAL ADVISORY COMMITTEE FOR AERONAUTICS

TECHNICAL NOTE NO. 1193

EFFECT OF PRODUCT OF INERTIA ON LATERAL STABILITY

By Leonard Sternfield

SUMMARY

A theoretical investigation was made to determine the effect of the product-of-inertia terms in the lateral equations of motion on the lateral-stability boundaries. The product of inertia results from the inclination of the principal longitudinal axis of the airplane to the flight path.

The results of the calculations indicated that the product-of-inertia terms should be included in the lateral equations of motion to determine the lateral stability of an airplane. The value of the directional-stability derivative C_{n_β} required for stability, as determined from the calculations which include the product of inertia caused by the inclination of the principal longitudinal axis above the flight path, is considerably less than the value predicted by calculations neglecting the product-of-inertia terms. when Q is positive.

INTRODUCTION

Recent flight tests and tests in the Langley free-flight tunnel indicated a discrepancy between the observed and calculated conditions for dynamic lateral stability. It was suggested that the discrepancy might be the result of neglecting terms in the equations of motion involving the product of inertia.

The theoretical investigations of the lateral stability of airplanes undertaken in the past have for the most part neglected the effect of the inclination of the principal longitudinal axis of the airplane to the flight path on the oscillatory-stability boundary. (See references 1 to 3.) In the appendix of reference 1, Zimmerman mentions that the results of supplementary calculations indicated that to neglect the angularity of the principal axis to the flight path did not seriously affect the oscillatory-stability boundary in the normal-flight range and gave slightly conservative results. The results of reference 1, consequently, are based on lateral equations

of motion from which the effect of the inclination of the principal axis to the flight path are omitted, namely, the terms including the product of inertia.

For the range of airplane parameters investigated by Zimmerman, the product-of-inertia terms probably have a small stabilizing effect on the oscillatory-stability boundary. However, the effect of product of inertia on the results of stability calculations covering the range of parameters of present-day airplanes designed for high-speed, high-altitude flight - that is, high values of the relative-density factor μ, a large increase in the effective-dihedral parameter C_{l_β} caused by the use of swept-back wings, and the change in the mass distribution of the airplane - has not been investigated.

In the present investigation, calculations were made to determine the effect of the product of inertia on the requirements for lateral stability. The results of the computations were plotted as a function of the directional-stability derivative C_{n_β} and the effective-dihedral parameter C_{l_β}.

SYMBOLS

V	airspeed, feet per second
ρ	mass density of air, slugs per cubic foot
q	dynamic pressure, pounds per square foot $\left(\frac{1}{2}\rho V^2\right)$
b	wing span, feet
S	wing area, square feet
W	weight of airplane, pounds
m	mass, slugs (W/g)
g	acceleration of gravity, feet per second per second
μ	relative-density factor $\left(\frac{m}{\rho S b}\right)$
k_{X_o}	radius of gyration about principal longitudinal axis, feet

k_{Z_o} radius of gyration about principal normal axis, feet

I_{X_o} moment-of-inertia coefficient about principal longitudinal axis

I_{Z_o} moment-of-inertia coefficient about principal normal axis

I_X moment-of-inertia coefficient about flight-path axis

I_Z moment-of-inertia coefficient about axis normal to flight path

I_{XZ} product-of-inertia coefficient with respect to flight path and axis normal to flight path

C_L lift coefficient $\left(\frac{W}{qS}\cos\gamma\right)$

C_l rolling-moment coefficient $\left(\frac{\text{Rolling moment}}{qSb}\right)$

C_n yawing-moment coefficient $\left(\frac{\text{Yawing moment}}{qSb}\right)$

C_Y lateral-force coefficient $\left(\frac{\text{Lateral force}}{qS}\right)$

ϕ angle of bank, radians

ψ azimuth angle, radians

β angle of sideslip, radians

$r, \dot{\psi}$ yawing angular velocity, radians per second $(d\psi/dt)$

$p, \dot{\phi}$ rolling angular velocity, radians per second $(d\phi/dt)$

C_{l_β} effective-dihedral derivative, rate of change of rolling-moment coefficient with angle of sideslip, per radian $\left(\partial C_l/\partial\beta\right)$

C_{n_β} directional-stability derivative, rate of change of yawing-moment coefficient with angle of sideslip, per radian $\left(\partial C_n/\partial\beta\right)$

C_{Y_β} lateral-force derivative, rate of change of lateral-force coefficient with angle of sideslip, per radian $\left(\partial C_Y/\partial\beta\right)$

C_{n_r} damping-in-yaw derivative, rate of change of yawing-moment coefficient with yawing-angular-velocity factor, per radian $\left(\partial C_n/\partial\frac{rb}{2V}\right)$

C_{l_p} damping-in-roll derivative, rate of change of rolling-moment coefficient with rolling-angular-velocity factor, per radian $\left(\partial C_l/\partial\frac{pb}{2V}\right)$

C_{n_p} rate of change of yawing-moment coefficient with rolling-angular-velocity factor, per radian $\left(\partial C_n/\partial\frac{pb}{2V}\right)$

C_{l_r} rate of change of rolling-moment coefficient with yawing-angular-velocity factor, per radian $\left(\partial C_l/\partial\frac{rb}{2V}\right)$

C_{Y_p} rate of change of lateral-force coefficient with rolling-angular-velocity factor, per radian $\left(\partial C_Y/\partial\frac{pb}{2V}\right)$

C_{Y_r} rate of change of lateral-force coefficient with yawing-angular-velocity factor, per radian $\left(\partial C_Y/\partial\frac{rb}{2V}\right)$

t time, seconds

D differential operator (d/dt)

Λ angle of sweepback, degrees

η angle of attack of principal longitudinal axis of airplane, positive when principal axis is above flight path, degrees (see fig. 1)

γ angle of flight path to horizontal, positive in a climb, degrees (see fig. 1)

θ angle between reference axis and horizontal, positive when reference axis is above horizontal, degrees (see fig. 1)

ϵ angle between reference axis and principal axis, positive when reference axis is above principal axis, degrees (see fig. 1)

R Routh's discriminant

EQUATIONS OF MOTION

The linearized equations of motion, referred to the axes in figure 1, used to calculate the spiral- and oscillatory-stability boundaries for any flight condition, are:

Rolling

$$\left[\left(I_{X_o}\cos^2\eta + I_{Z_o}\sin^2\eta\right)D^2 - C_{l_{\dot{\phi}}}D\right]\phi$$

$$-\left[-\left(I_{Z_o} - I_{X_o}\right)\sin\eta\cos\eta\,D^2 + C_{l_{\dot{\psi}}}D\right]\psi - C_{l_\beta}\beta = 0$$

Yawing

$$\left[\left(I_{Z_o}\cos^2\eta + I_{X_o}\sin^2\eta\right)D^2 - C_{n_{\dot{\psi}}}D\right]\psi$$

$$-\left[-\left(I_{Z_o} - I_{X_o}\right)\sin\eta\cos\eta\,D^2 + C_{n_{\dot{\phi}}}D\right]\phi - C_{n_\beta}\beta = 0$$

Sideslipping

$$\frac{2b\mu}{V}(D\psi + D\beta) - \left(C_L + C_{Y_{\dot{\phi}}}D\right)\phi - \left(C_L\tan\gamma + C_{Y_{\dot{\psi}}}D\right)\psi - C_{Y_\beta}\beta = 0$$

where

$$I_{X_o} = \frac{mk_{X_o}^2}{qbS}$$

$$I_{Z_o} = \frac{mk_{Z_o}^2}{qbS}$$

$$C_{l_{\dot{\phi}}} = C_{l_p}\left(\frac{b}{2V}\right)$$

$$C_{l_{\dot{\psi}}} = C_{l_r}\left(\frac{b}{2V}\right)$$

$$C_{n_{\dot{\phi}}} = C_{n_p}\left(\frac{b}{2V}\right)$$

$$C_{n_{\dot{\psi}}} = C_{n_r}\left(\frac{b}{2V}\right)$$

$$C_{Y_{\dot{\phi}}} = C_{Y_p}\left(\frac{b}{2V}\right)$$

and

$$C_{Y_{\dot{\psi}}} = C_{Y_r}\left(\frac{b}{2V}\right)$$

The symbols I_{X_o} and I_{Z_o} represent the moments of inertia about the principal axes of the airplane. If the longitudinal principal axis is inclined at an angle η to the flight path, the moments of inertia about the flight-path axis and the axis normal to the flight path are:

$$I_X = I_{X_o} \cos^2\eta + I_{Z_o} \sin^2\eta$$

$$I_Z = I_{Z_o} \cos^2\eta + I_{X_o} \sin^2\eta$$

and the product of inertia is $I_{XZ} = -\left(I_{Z_o} - I_{X_o}\right) \sin\eta \cos\eta$.

$$-\frac{(I_z - I_x)\sin\eta\cos\eta}{\cos^2\eta - \sin^2\eta} = -\frac{1}{2}(I_z - I_x)\tan 2\eta$$

When $\phi_o e^{\lambda t}$ is substituted for ϕ, $\psi_o e^{\lambda t}$ for ψ, and $\beta_o e^{\lambda t}$ for β in the equations written in determinant form, λ must be a root of the equation

$$A\lambda^4 + B\lambda^3 + C\lambda^2 + E\lambda + F = 0$$

where

$$A = -I_{XZ}^2 \frac{2b\mu}{V} + I_X I_Z \frac{2b\mu}{V}$$

$$B = -I_{XZ} C_{l_{\dot{\psi}}} \frac{2b\mu}{V} + I_{XZ}^2 C_{Y_\beta} - I_{XZ} C_{n_{\dot{\phi}}} \frac{2b\mu}{V} - I_X C_{n_{\dot{\psi}}} \frac{2b\mu}{V}$$

$$- I_Z \frac{2b\mu}{V} C_{l_{\dot{\phi}}} - I_X I_Z C_{Y_\beta}$$

$$C = I_{XZ} C_{Y_\beta} C_{l_{\dot{\psi}}} + I_{XZ} \frac{2b\mu}{V} C_{l_\beta} + I_{XZ} C_{Y_\beta} C_{n_{\dot{\phi}}} + I_X C_{Y_\beta} C_{n_{\dot{\psi}}}$$

$$+ I_X \frac{2b\mu}{V} C_{n_\beta} + I_Z C_{l_{\dot{\phi}}} C_{Y_\beta} + \frac{2b\mu}{V} C_{l_{\dot{\phi}}} C_{n_{\dot{\psi}}} - \frac{2b\mu}{V} C_{n_{\dot{\phi}}} C_{l_{\dot{\psi}}}$$

$$- I_{XZ} C_{Y_{\dot{\phi}}} C_{n_\beta} - I_Z C_{Y_{\dot{\phi}}} C_{l_\beta} - I_X C_{Y_{\dot{\psi}}} C_{n_\beta} - I_{XZ} C_{Y_{\dot{\psi}}} C_{l_\beta}$$

$$E = -I_{XZ} C_{n_\beta} C_L - I_Z C_{l_\beta} C_L - C_{l_{\dot{\phi}}} C_{n_{\dot{\psi}}} C_{Y_\beta} - C_{l_{\dot{\phi}}} C_{n_\beta} \frac{2b\mu}{V}$$

$$+ C_{n_{\dot{\phi}}} C_{l_{\dot{\psi}}} C_{Y_\beta} + C_{n_{\dot{\phi}}} C_{l_\beta} \frac{2b\mu}{V} - I_{XZ} C_{l_\beta} C_L \tan\gamma - I_X C_{n_\beta} C_L \tan\gamma$$

$$- C_{Y_{\dot{\phi}}} C_{l_{\dot{\psi}}} C_{n_\beta} + C_{Y_{\dot{\phi}}} C_{n_{\dot{\psi}}} C_{l_\beta} + C_{Y_{\dot{\psi}}} C_{l_{\dot{\phi}}} C_{n_\beta} - C_{Y_{\dot{\psi}}} C_{n_{\dot{\phi}}} C_{l_\beta}$$

$$F = C_L \left(C_{l_\beta} C_{n_{\dot{\psi}}} - C_{l_{\dot{\psi}}} C_{n_\beta} \right) + C_L \tan\gamma \left(C_{n_\beta} C_{l_{\dot{\phi}}} - C_{l_\beta} C_{n_{\dot{\phi}}} \right)$$

The conditions necessary to obtain the oscillatory-stability boundary are that the coefficients A, B, C, and E must be positive and Routh's discriminant, $R = BCE - AE^2 - B^2F$, must equal zero. The spiral-stability boundary is found by setting $F = 0$. The completely stable region is therefore bounded by the curves $R = 0$ and $F = 0$, which are plotted as a function of the directional-stability derivative C_{n_β} and the effective-dihedral derivative C_{l_β}.

Stability Derivatives and Mass Characteristics

Calculations were made showing the effect of the product-of-inertia terms on the oscillatory-stability boundary for a hypothetical supersonic fighter airplane, an experimental fighter airplane, and a model flown in the Langley free-flight tunnel. The values of the stability derivatives and mass characteristics of the two airplanes and the model are given in table I. The contribution of the tail to the derivatives C_{n_p} and C_{l_r} (see reference 2) was included in the characteristics of the experimental fighter airplane and the free-flight-tunnel model but was neglected in the calculations of the hypothetical supersonic fighter airplane.

RESULTS AND DISCUSSION

The results of the investigation are presented in a series of figures which show the oscillatory- and spiral-stability boundaries as a function of C_{n_β} and C_{l_β}. The solid $R = 0$ curve of figure 2 represents the oscillatory-stability boundary for landing flight for a hypothetical supersonic fighter airplane which has its principal axis or fuselage inclined 5° above the flight path but the product of inertia I_{XZ} is assumed to be zero. The dashed curve in this figure is the $R = 0$ boundary for the same condition with the product-of-inertia terms included in the equations of motion. A comparison of both curves shows a large stabilizing shift in the oscillatory-stability boundary for the case in which the product of inertia is taken into account. As C_{l_β} is increased, the value of C_{n_β} required for oscillatory stability as determined by the calculations including I_{XZ} is considerably less than the value determined by the calculations neglecting I_{XZ}. The spiral-stability boundary plotted in figure 2 and in subsequent figures applies to both sets of calculations since this boundary is not a

function of the product of inertia. This result does not mean, however, that the rate of divergence or convergence of the spiral motion will be the same inasmuch as the stability equation is different in each case. The effect of I_{XZ} on the $R = 0$ boundary for the same airplane in cruising flight is presented in figure 3. The solid curve represents the case of the principal longitudinal axis inclined 2° either above or below the flight path but neglects the effect of I_{XZ}. The other two $R = 0$ boundaries that were calculated included the effect of product of inertia. For the case in which the principal axis is inclined above the flight path, $I_{XZ} = -0.00178$, the stable region is increased; whereas for the case in which the principal axis is inclined below the flight path, $I_{XZ} = 0.00178$, the stable region is reduced.

The experimental fighter airplane and the free-flight-tunnel model were tested in flight with the principal axis inclined 16° and 10°, respectively, above the flight path. The initial calculations made on the assumption that $I_{XZ} = 0$ (the solid curves in figs. 4 and 5) indicated that the airplane and model would be unstable in flight for the combination of C_{n_β} and C_{l_β} denoted by the circled points in figures 4 and 5. The flight-test results, however, showed that the experimental fighter airplane was stable and the free-flight-tunnel model was marginally stable. Subsequent calculations which included the product-of-inertia terms indicated that the $R = 0$ boundary for the experimental fighter airplane increased the stable region to include the combination of C_{n_β} and C_{l_β} tested in flight and that the $R = 0$ boundary for the free-flight-tunnel model was shifted very close to the marginally stable test point.

In general, the inclination of the principal longitudinal axis above the flight path causes a stabilizing shift in the oscillatory-stability boundary but the extent of the shift is a function of other airplane parameters which are still to be investigated.

The solid curves of figures 2 to 5 may be considered to represent the $R = 0$ boundary for the actual flight conditions of an airplane which has its principal longitudinal axis in line with the flight path ($I_{XZ} = 0$) provided the wings are set at an angle of incidence to the fuselage to obtain the lift coefficient desired for flight. The dashed curve on each figure would, therefore, represent the $R = 0$ boundary for the same flight conditions as the solid curve but with the wings set at a different angle of incidence

since the principal axis is inclined to the flight path. If the principal axis is inclined above the flight path, the angle of incidence which corresponds to the dashed curve is smaller than the angle of incidence corresponding to the solid curve. If the principal axis is inclined below the flight path, however, the wing incidence is larger than the wing incidence of the airplane in which the principal axis coincides with the flight path. For example, the solid curve of figure 2 is the $R = 0$ boundary for an airplane with the wings set at an angle of 15° to the fuselage and the principal axis in line with the flight path; whereas the dashed curve is the $R = 0$ boundary for the same airplane with the wings set at a 10° angle of incidence and the principal axis inclined 5° above the flight path. In figure 3, the wing incidence is 7° for the solid curve, 5° for the case of the principal axis above the flight path, and 9° for the case of the principal axis below the flight path. The solid curves of figures 4 and 5 are the $R = 0$ boundaries for the airplane and model designed with a wing incidence of 16° and 10°, respectively; for both cases the dashed curve represents an airplane with a wing incidence of 0°. This interpretation applied to the solid curves of figures 4 and 5 is only approximately true since the angle of attack at the tail is zero if the wing is at 16° or 10° incidence and the principal axis coincides with the line of flight; whereas the calculations include the effect of the tail at an angle of attack of 16° and 10° on the stability derivatives C_{n_p} and C_{l_r}.

A comparison of the solid and dashed curves in each figure clearly indicates the increase in the oscillatory-stability region for an airplane designed with a wing set at 0° incidence, thereby necessitating the inclination of the principal axis above the flight path to obtain the desired lift coefficient.

CONCLUDING REMARKS

The results of the analysis made to investigate the effect of the product of inertia on the lateral-stability boundaries emphasize the necessity of including the product-of-inertia terms in the lateral equations of motion to determine the lateral stability of an airplane. The calculations indicate that the inclination of the principal longitudinal axis above the flight path causes a stabilizing shift in the oscillatory-stability boundary.

Langley Memorial Aeronautical Laboratory
National Advisory Committee for Aeronautics
Langley Field, Va., August 13, 1946

REFERENCES

1. Zimmerman, Charles H.: An Analysis of Lateral Stability in Power-Off Flight with Charts for Use in Design. NACA Rep. No. 589, 1937.

2. Bamber, Millard J.: Effect of Some Present-Day Airplane Design Trends on Requirements for Lateral Stability. NACA TN No. 814, 1941.

3. Bryant, L. W., and Pugsley, A. G.: The Lateral Stability of Highly Loaded Aeroplanes. R.& M. No. 1840, British A.R.C., 1938.

TABLE I

STABILITY DERIVATIVES AND MASS CHARACTERISTICS USED IN STABILITY CALCULATIONS

	Hypothetical supersonic fighter airplane		Experimental fighter airplane	Free-flight-tunnel model
Condition	Landing	Cruising	Landing	Landing
W/S, lb/sq ft	80	80	35	1.85
b, ft	20	20	34	3.8
ρ, slugs/cu ft	0.00238	0.0002	0.00238	0.00238
V, ft/sec	264	1465	173	44
C_L	1	0.372	1	0.8
μ	54	620	13	6.33
k_{X_o}, ft	2.02	2.02	5.28	0.51
k_{Z_o}, ft	9.64	9.64	8.03	1.29
C_{l_p}, per radian	-0.197	-0.197	-0.3	-0.17
C_{l_r}, per radian	0.25	0.0929	$0.25 - 0.04C_{n_{\beta(tail)}}$	$0.142 - 0.099C_{n_{\beta(tail)}}$
C_{n_p}, per radian	-0.0198	-0.00732	$-0.029 - 0.04C_{n_{\beta(tail)}}$	$-0.0406 - 0.099C_{n_{\beta(tail)}}$
C_{n_r}, per radian	$-1.47C_{n_{\beta(tail)}}$	$-1.47C_{n_{\beta(tail)}}$	$-0.086 - 0.858C_{n_{\beta(tail)}}$	$-0.0131 - 1.2C_{n_{\beta(tail)}}$
C_{Y_p}, per radian	0	0	0	0
C_{Y_r}, per radian	0	0	0	0
C_{Y_β}, per radian	$-1.33C_{n_{\beta(tail)}}$	$-1.33C_{n_{\beta(tail)}}$	$-0.43 - 2.34C_{n_{\beta(tail)}}$	$-0.0074 - 1.76C_{n_{\beta(tail)}}$
$C_{n_{\beta(fuselage)}}$, per radian	-0.25	-0.25	-0.02	0
γ, deg	0	0	0	-9
Λ, deg	60	60	35	42

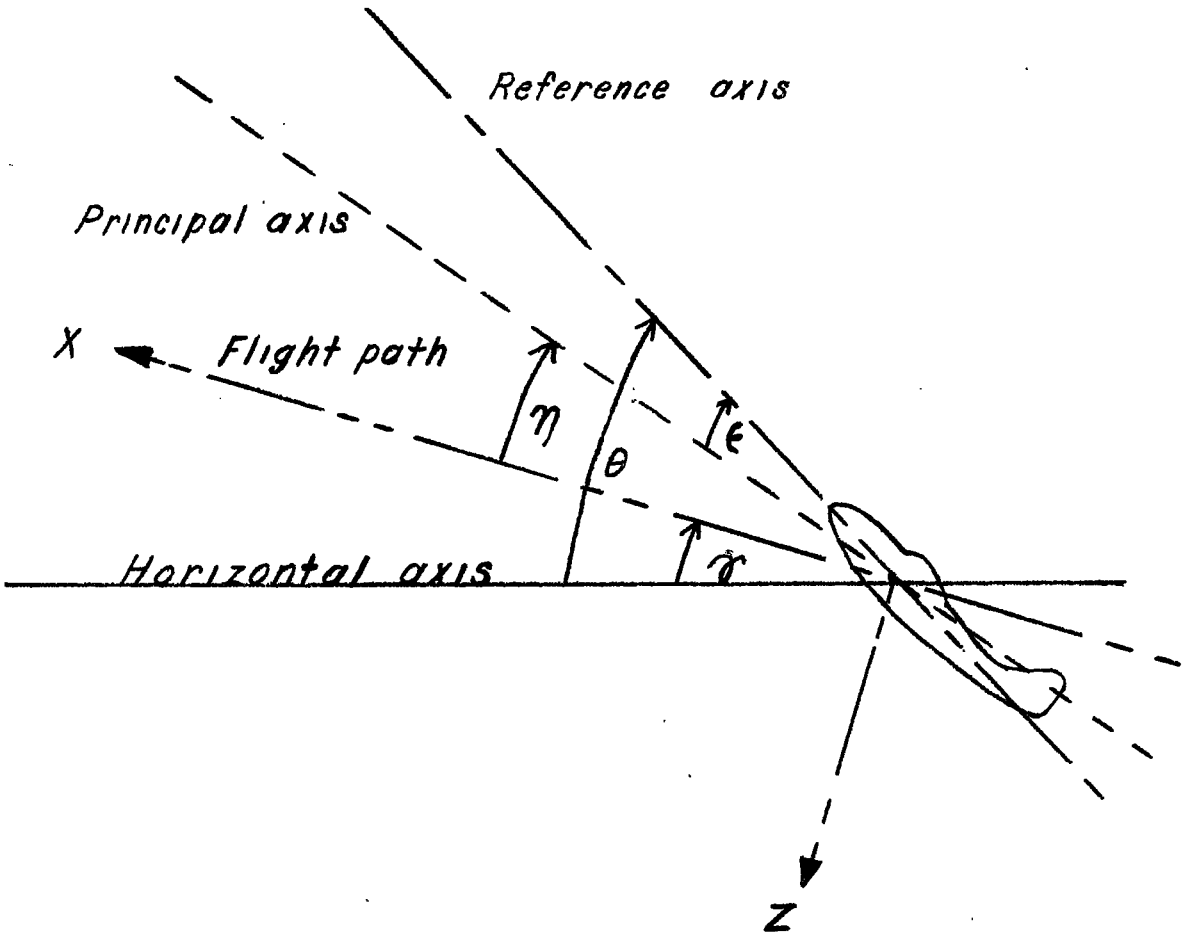

Figure 1.— System of axes and angular relationships in flight. Arrows indicate positive direction of angles. $\eta = \theta - \gamma - \epsilon$

NATIONAL ADVISORY
COMMITTEE FOR AERONAUTICS

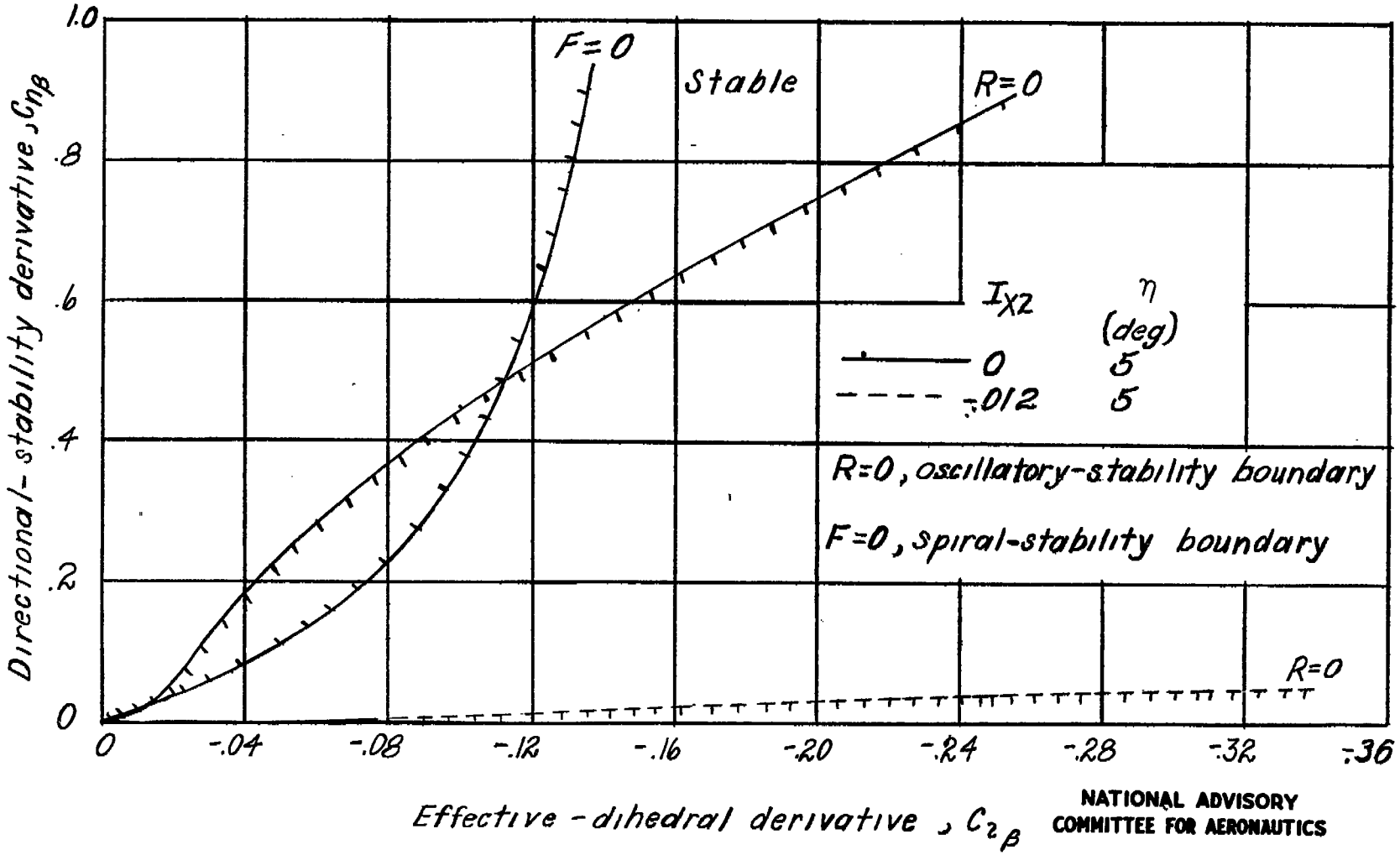

Figure 2.- Lateral-stability boundaries for landing flight for hypothetical supersonic fighter airplane.

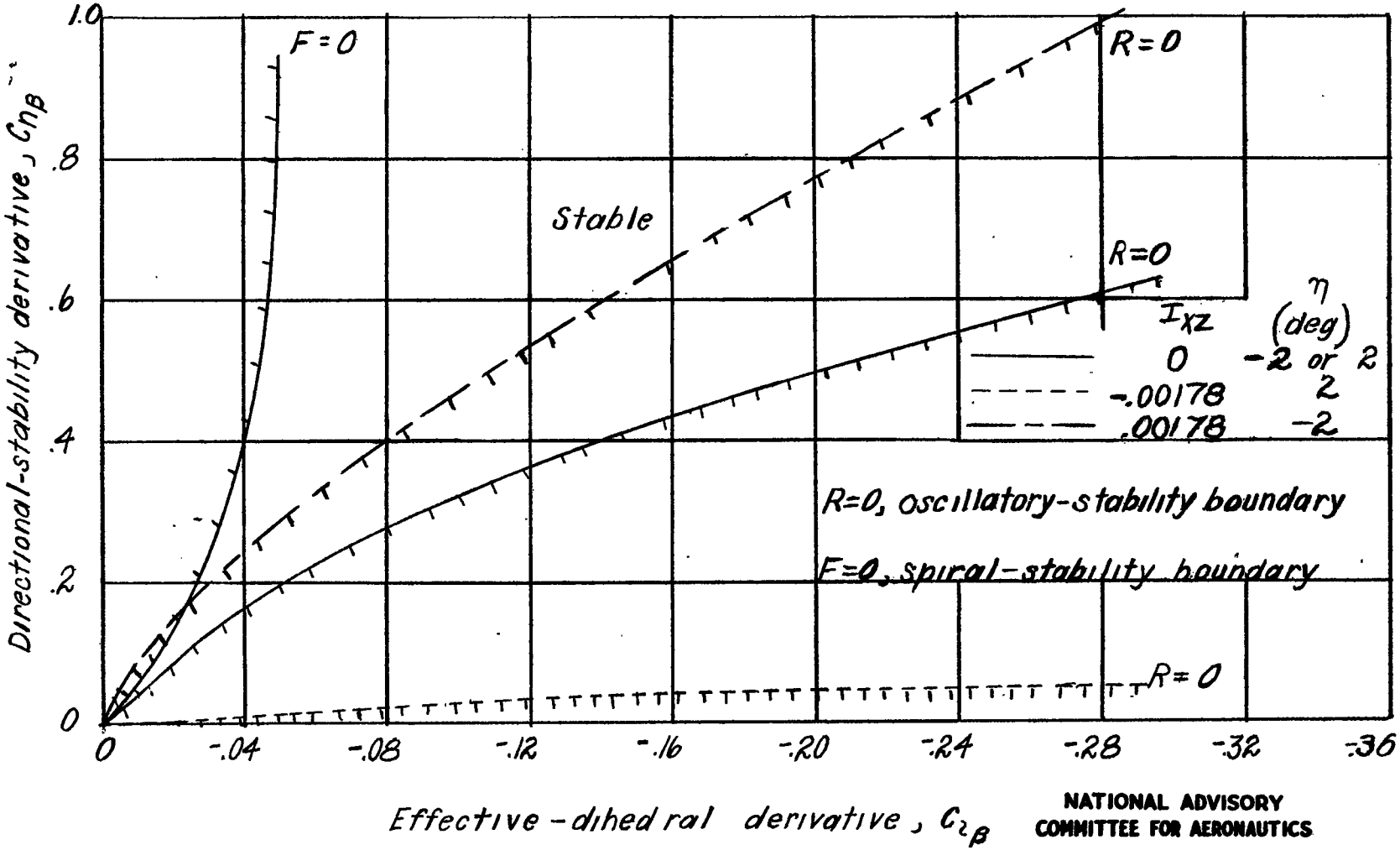

Figure 3.— Lateral-stability boundaries for cruising flight for hypothetical supersonic fighter airplane.

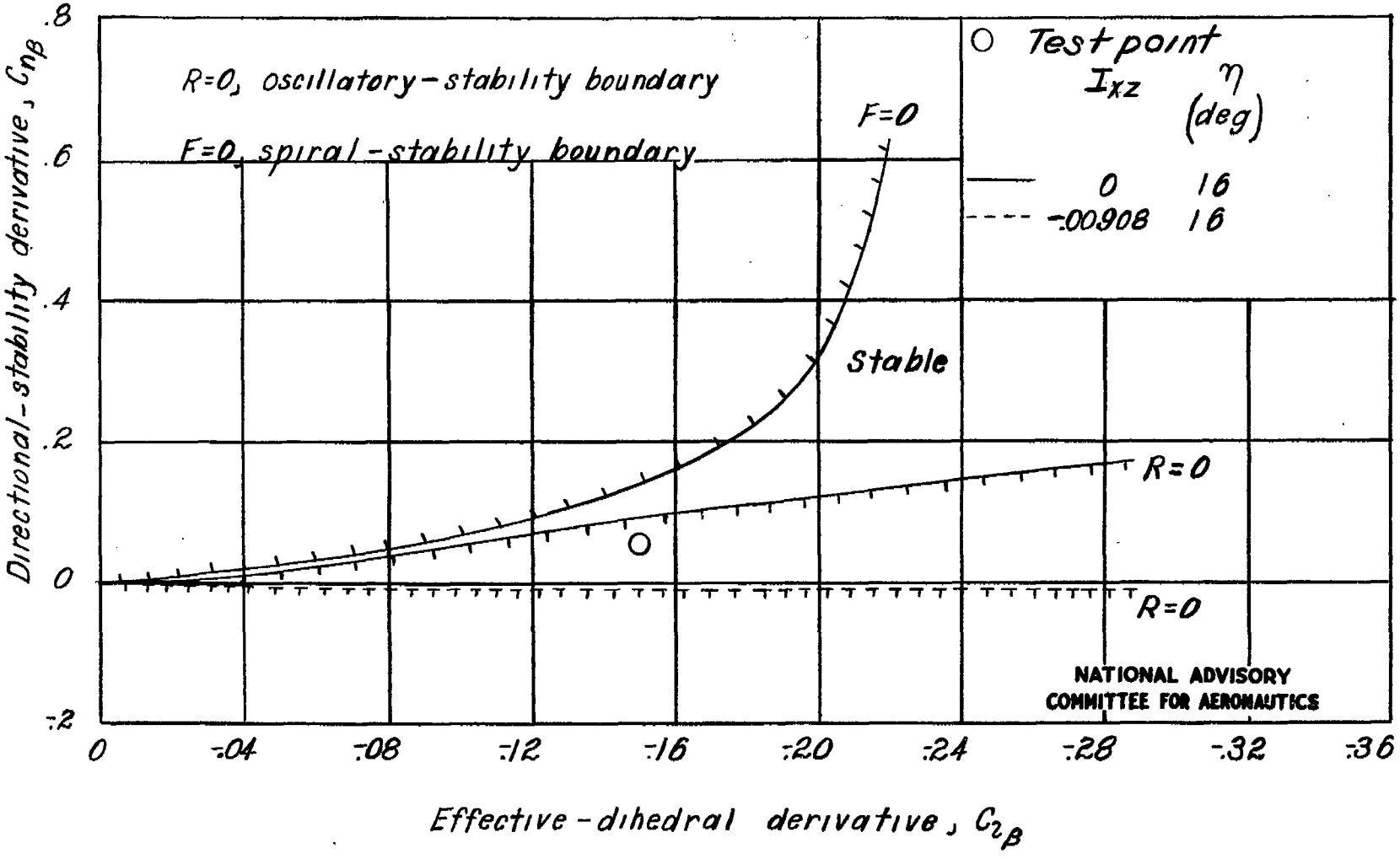

Figure 4.— Lateral-stability boundaries for landing flight for experimental fighter airplane.

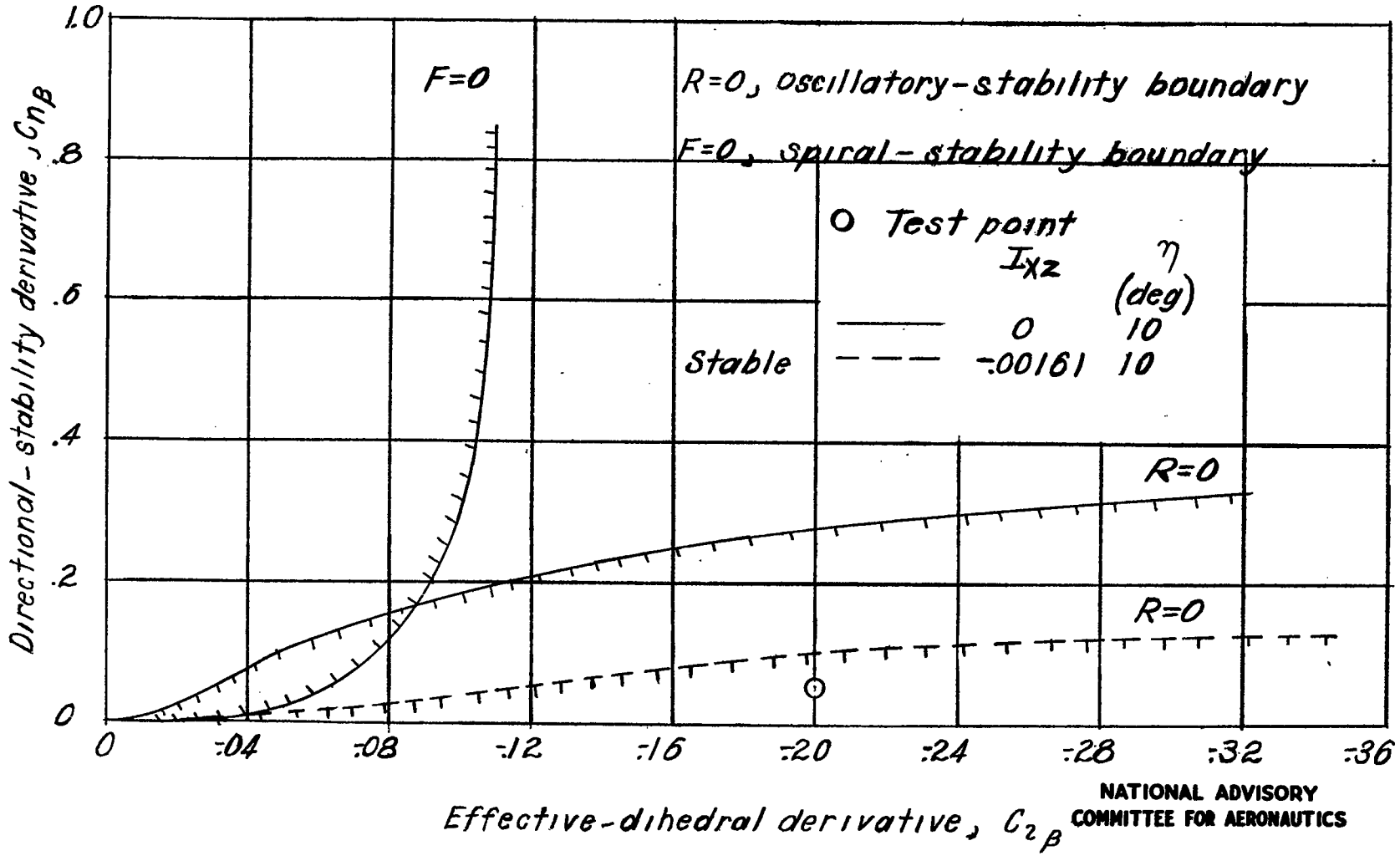

Figure 5.— Lateral-stability boundaries for landing flight for free-flight-tunnel model.